

ELMO2 association with Gαi2 regulates pancreatic cancer cell chemotaxis and metastasis

Yecheng Wang¹, Hongyan Li¹, Fei Li^{Corresp. 1}

¹ Department of General Surgery, Xuanwu Hospital Capital Medical University, Bei Jing, China

Corresponding Author: Fei Li
Email address: xw_lifei36@163.com

Background. Pancreatic cancer is a highly lethal disease. Nearly half of the patients have distant metastasis and remain asymptomatic. Emerging evidence suggests that the chemokine, CXCL12, has a role in cancer metastasis. The interaction between CXCL12 and CXCR4 activates heterotrimeric G proteins, which regulates actin polymerization and cancer cell migration. However, the molecular mechanisms underlying pancreatic cancer cell migration are still largely obscure. Here, we addressed the role of ELMO2 in chemotaxis and metastasis of pancreatic cancer cells.

Methods. Pancreatic cancer cell lines PANC-1 and AsPC-1 and siRNA-mediated knockdown of ELMO2 were used to determine the effects of ELMO2 on cancer cell chemotaxis, invasion, migration. Co-immunoprecipitation assays were carried out to identify interacting partners of ELMO2.

Results. ELMO2 knockdown inhibited pancreatic cancer cell chemotaxis, migration, invasion, and F-actin polymerization. Co-immunoprecipitation assays revealed that ELMO2 interacted with Gαi2 and that CXCL12 triggered Gαi2-dependent membrane translocation of ELMO2. Thus, ELMO2 is a potential therapeutic target for pancreatic cancer.

1 ELMO2 Association with Gai2 Regulates Pancreatic Cancer 2 Cell Chemotaxis and Metastasis

3

4 Yecheng Wang¹, Hongyan Li¹, Fei Li¹5 ¹ Department of General Surgery, Xuanwu Hospital, Capital Medical University, Beijing, China

6 Corresponding author:

7 Fei Li

8 Xuanwu Hospital, Capital Medical University, Beijing 100053, China

9 Email: xw_lifei36@163.com

10

11 Abstract

12 **Background.** Pancreatic cancer is a highly lethal disease. Nearly half of the patients have distant
13 metastasis and remain asymptomatic. Emerging evidence suggests that the chemokine, CXCL12,
14 has a role in cancer metastasis. The interaction between CXCL12 and CXCR4 activates
15 heterotrimeric G proteins, which regulates actin polymerization and cancer cell migration.
16 However, the molecular mechanisms underlying pancreatic cancer cell migration are still largely
17 obscure. Here, we addressed the role of ELMO2 in chemotaxis and metastasis of pancreatic
18 cancer cells.

19 **Methods.** Pancreatic cancer cell lines PANC-1 and AsPC-1 and siRNA-mediated knockdown of
20 ELMO2 were used to determine the effects of ELMO2 on cancer cell chemotaxis, invasion,
21 migration. Co-immunoprecipitation assays were carried out to identify interacting partners of
22 ELMO2.

23 **Results.** ELMO2 knockdown inhibited pancreatic cancer cell chemotaxis, migration, invasion,
24 and F-actin polymerization. Co-immunoprecipitation assays revealed that ELMO2 interacted
25 with Gai2 and that CXCL12 triggered Gai2-dependent membrane translocation of ELMO2.
26 Thus, ELMO2 is a potential therapeutic target for pancreatic cancer.

27

28 **Keywords:** Pancreatic cancer, ELMO2, Gai2, Metastasis, Cell migration, Chemotaxis

29

30 Introduction

31 Pancreatic cancer is one of the most malignant cancers of the digestive system. Currently, it is
32 the fourth leading cause of cancer-related death due to early invasion and rapid metastasis
33 (Kleeff et al. 2016; Siegel et al. 2018). Because of the lack of reliable markers for early diagnosis
34 and aggressive tumor biology, the 5-year overall survival rate is still extremely low, and, despite
35 important clinical advancements, the outcome is unfavorable in most patients (Conroy et al.
36 2016; Garrido-Laguna & Hidalgo 2015). Therefore, it is of vital importance to discover and
37 characterize the molecular mechanisms underlying pancreatic cancer cell migration and

38 metastasis. This may help identify novel factors involved in multi-step tumor metastasis and
39 improve the treatments.

40 ELMO (Engulfment and Cell Motility) is a family of related scaffold proteins involved in
41 intracellular signaling networks and with a high degree of evolutionary conservation. In
42 mammals, the ELMO protein family consists of three isoforms: ELMO1, ELMO2, and ELMO3.
43 As the mammalian homologs of *Caenorhabditis elegans* CED-12, the ELMO proteins play a
44 major role in cell migration and cytoskeletal rearrangements (Gumienny et al. 2001). Although
45 they lack intrinsic catalytic activity, ELMO proteins can function as adaptors to regulate the
46 activity of plasma membrane and cytoplasmic proteins (Patel et al. 2011). Previous studies have
47 shown that ELMO protein interactions with a number of different proteins activate signaling
48 pathways that cause cell migration or promote cell movement. Proteins interacting with ELMO,
49 such as Gai2, Gβγ, and Nck-1, are mostly cell membrane-associated and involved in the
50 regulation of cytoskeletal organization (Fritsch et al. 2013; Li et al. 2013; Zhang et al. 2014).
51 Interestingly, ELMO family members such as ELMO1 and ELMO3 have been implicated in a
52 variety of malignant cancers, such as glioma, breast cancer, colorectal cancer, hepatocellular
53 carcinoma, and non-small-cell lung carcinoma (Fan et al. 2015; Jarzynka et al. 2007; Jiang et al.
54 2011; Peng et al. 2016; Zhang et al. 2015). In previous studies, the researches mostly focused on
55 the function of ELMO1 and EMLO3 in tumor development, invasion, and formation of
56 metastasis. However, the studies about the role and function of ELMO2 were very few. Early
57 reports only showed that ELMO2 localized to cell–cell contacts regulating both integrin- and
58 cadherin-based adhesions, which facilitated to reposition the cells from migration to strong cell–
59 cell adhesion (Toret et al. 2014). Unfortunately, the biological behaviors and molecular
60 mechanisms of ELMO2 remained unclear. To our knowledge no previous studies have illustrated
61 a relationship between ELMO2 and invasiveness in pancreatic cancer. This study aimed to fully
62 understand the function and mechanisms of ELMO2 in pancreatic cancer chemotaxis and
63 metastasis.

64 G proteins, also known as guanine nucleotide-binding proteins, are a family of molecular
65 transducers involved in the transmission of signals generated by a variety of stimuli, such as
66 chemokines, neurotransmitters, and hormones. G proteins are typically represented by the
67 membrane-associated heterotrimeric G proteins, which are activated by G protein-coupled
68 receptors (GPCRs), and are engaged in cell signaling. Heterotrimeric G proteins consist of three
69 major subunits, alpha (α), beta (β), and gamma (γ). During the past two decades, the function of
70 G proteins has been extensively investigated. Signaling molecules like chemokines bind to the
71 extracellular GPCR domain, after which an intracellular domain facilitates the dissociation of the
72 heterotrimeric G proteins, Gai and Gβγ, which in turn activates a cascade of intracellular
73 signaling events (Fraser 2008; Xu et al. 2010). GPCRs and G proteins may cooperate in the
74 regulation of cell actin cytoskeleton. The accumulation of actin filaments at leading-edge
75 protrusions of the cell membrane increases cell mobility and promotes cell migration (Hurst &
76 Hooks 2009; Kim et al. 2013; Muller et al. 2001). However, little information is available on the
77 role of G proteins in the migration and metastasis of pancreatic cancer cells.

78 In metastasis, cancer cells detach from the primary tumor, travel through the bloodstream or

79 lymph system, and form a new tumor in other organs or tissues. To metastasize or spread, cancer
80 cells need to invade, escape from a proper vessel, and settle at a distant site (Condeelis & Segall
81 2003). Chemotaxis is the movement of an organism or cell in response to a chemical stimulus
82 (Iglesias & Devreotes 2008). Chemokines are a family of small cytokines, signaling proteins
83 secreted by a variety of cells. They induce chemotaxis by interacting with specific chemokine
84 receptors on the surfaces of target cells. The crucial role of chemotaxis in the recruitment of
85 inflammatory cells to infection sites is a long-established concept (Jin et al. 2009). Interestingly,
86 recent studies have shown that chemotaxis is critical for cancer cell dissemination (Condeelis et
87 al. 2005; Murphy 2001). A complex network of chemokines contributes to chemotaxis in tumor
88 cells, regulating cancer cell growth, invasion, and metastatic progression (Balkwill 2004;
89 Swaney et al. 2010). A particularly important role in chemotaxis is played by the chemokine
90 receptor, CXCR4, and by its ligand, CXCL12 (also known as SDF1, stromal cell-derived factor
91 1), which initiate directed cell migration in various kinds of cancer (Archibald et al. 2012; Hu et
92 al. 2014; Li et al. 2014; Yang et al. 2015). The CXCR4/CXCL12 interaction triggers downstream
93 signaling cascades that may promote metastatic progression (Guyon 2014). However, the
94 molecular mechanism by which this complex affects metastasis in pancreatic cancer remains to
95 be elucidated.

96 In this study, we investigated the role of ELMO2 and CXCL12 in pancreatic cancer using cancer
97 cell lines. The results of this study are expected to provide novel insights into the metastatic
98 progression of pancreatic cancer cells.

99

100 **Materials & Methods**

101

102 **Cell Culture**

103 The pancreatic cancer cell lines, PANC-1 and AsPC-1, were purchased from American Type
104 Culture Collection (Manassas, VA, USA). All pancreatic cancer cell lines were cultured in
105 RPMI-1640 medium (Hyclone, Shanghai, China) supplemented with 10% fetal bovine serum
106 (FBS; Gibco Invitrogen Corporation, Australia) and were incubated at 37 °C in a humidified
107 atmosphere containing 5% CO₂.

108

109 **Western blotting**

110 After indicated treatments, cells were collected and total proteins were extracted with PMSF
111 (Beyotime Biotechnology, shanghai, China) containing RIPA lysis buffer (Beyotime
112 Biotechnology, shanghai, China) as instructed. Protein samples were quantified by Pierce™
113 BCA Protein Assay Kit (Thermo Scientific) via spectrophotometer (Thermo Scientific, USA) at
114 562 nm. Protein loading buffer (Sigma) was applied to denature protein samples. Total protein
115 samples (20 µg/lane) were separated by 10% sodium dodecyl sulfate polyacrylamide gel
116 electrophoresis (SDS-PAGE), and transferred to a polyvinylidene difluoride membrane (GE
117 Healthcare Amersham™ Hybond™). The membranes were blocked with 5% skim milk for one
118 hour at room temperature and incubated with the primary antibodies anti-ELMO2 (ab2240,

119 Abcam), anti-Gai2 (sc-13534, Santa Cruz Biotechnology) or anti-GAPDH (ab8245, Abcam) at 4
120 °C overnight, and then were washed three times with PBS containing 0.1% Tween-20 (PBST).
121 The membranes were then incubated with the horseradish peroxidase-conjugated secondary
122 antibodies anti-goat (ab6885, Abcam), anti-mouse (sc-516102, Santa Cruz Biotechnology) or
123 anti-rabbit (ab6721, Abcam) for 1 hour at room temperature. Finally, the bound proteins were
124 visualized using the SuperSignal™ West Pico PLUS Chemiluminescent Substrate (Thermo
125 Scientific) and analyzed with FluorChemHD2 system (ProteinSimple, USA).

126

127 **Transient Transfection**

128 Pancreatic cancer cell lines were cultured until they reached 60–80% of confluence before
129 transfection. To reduce the expression of ELMO2 and Gai2, specific siRNAs were used for in
130 vitro transfection. Cells were then incubated for 48 h, followed by protein expression analysis by
131 western blotting. The sequences of ELMO2 siRNA were 5'-
132 CCCAGAGUAAUUAUACCCUCCGUUAU-3', 5'-CCCACUACAGUGAGAUGCUGGCAUU-
133 3', and 5'-CACAUCAAUCCAGCCAUGGACUUUA-3'. The sequences of Gai2 siRNA were 5'-
134 GAGGACCUGAAUAAGCGCAAAGACA-3', 5'-ACGCCGUCACCGAUGUCAUCA-3', and
135 5'-CCGACACCAAGAACGUGCAGUUCGU-3'. To enhance the expression of ELMO2 and
136 Gai2, the overexpression plasmids GV362 and GV141, respectively, were transfected into
137 PANC-1 cells. Both plasmids were purchased from Genechem Co., Ltd (Shanghai, China). All
138 transfections were performed using Lipofectamine 3000 reagent (Invitrogen) in accordance with
139 the manufacturer's instructions. For the knockdown of ELMO2 throughout the studies, we chose
140 siRNA_1 whose sequence was 5'-CCCAGAGUAAUUAUACCCUCCGUUAU-3' to perform the
141 following experiments.

142

143 **Exogenous Co-immunoprecipitation (Co-IP)**

144 PANC-1 cells were plated in 10-cm culture dishes before transfection. To obtain a high level of
145 exogenous ELMO2 and Gai2 expression, PANC-1 cells were transfected with GV362 Flag-
146 ELMO2 and GV141 Flag-Gai2, respectively. Cells were collected and total proteins were
147 extracted with PMSF (Beyotime Biotechnology, shanghai, China) containing RIPA lysis buffer
148 (Beyotime Biotechnology, shanghai, China). First, we incubated the cell lysates with monoclonal
149 anti-flag antibodies (cat. F3165, Sigma) with continuous mixing overnight. Cell lysates were also
150 immunoprecipitated with control rabbit IgG antibodies (CST-2729, Cell Signaling Technology).
151 Next, PureProteome™ protein A/G mix magnetic beads (Merck-Millipore) were added to the
152 antibody-antigen complex and subjected to continuous mixing. Third, the precipitates were
153 eluted from the magnetic beads by boiling in electrophoresis sample buffer, separated by SDS-
154 PAGE, and detected with anti-Gai2 (sc-13534, Santa Cruz Biotechnology) and anti-ELMO2
155 (ab2240, Abcam) antibodies.

156

157 **Immunofluorescence**

158 Briefly, PANC-1 cells were plated in 24-well plates containing round glass coverslips (one per
159 well) and incubated for 24 h to obtain stable attachment to the glass coverslips. Before

160 stimulation with CXCL12 (R&D Systems, Inc.), cells were serum-starved for 3 h, followed by
161 incubation with CXCL12 (100 ng/ml) at 37 °C for 1 h. A solution containing 4%
162 paraformaldehyde was used for cell fixation. Cell membranes were permeabilized with 0.1%
163 Triton X-100. Donkey serum was used for blocking non-specific interactions, based on the
164 species in which the secondary antibody was raised. After the blocking step, cells were incubated
165 with diluted primary antibodies anti-ELMO2 (ab2240, Abcam) or anti-Gai2 (sc-13534, Santa
166 Cruz Biotechnology) overnight.
167 The cells were subsequently stained with Alexa Fluor 488-conjugated secondary antibody (cat.
168 A32814, Invitrogen) or 546-conjugated secondary antibody (cat. A10036, Invitrogen) for 1 h at
169 room temperature. Finally, cells on coverslips were mounted and visualized using a Leica TCS
170 SP5 II confocal microscope (Leica Microsystems CMS GmbH).

171

172 **Wound-Healing Assay**

173 Pancreatic cancer cell lines were seeded in 6-well plates and divided into three groups: normal,
174 control, and siELMO2. Cells were cultured until they reached an 80-90% density (ca. 24 h). The
175 cell monolayer was gently and slowly scratched with a 10- μ l pipette tip across the well. Then,
176 the wells were gently washed twice with PBS to remove the detached cells. The medium was
177 replaced by RPMI 1640 medium with 1% FBS. Finally, photographs of the monolayer were
178 taken with a microscope at various time points (0, 3, 6, 9, 12, and 24 h).

179

180 **Chemotaxis Assay**

181 The Chemotaxis assays were performed as described by the manufacturer (Neuro Probe) and by
182 Sun et al. (Sun et al. 2005). In this assay, a 48-well microchemotaxis chamber (AP48 chemotaxis
183 chamber, Neuro Probe) was used, and prepared 50 μ l cell suspension (2×10^5 cells per ml) were
184 placed on the upper chamber and were allowed to migrate through the permeable filter
185 membrane (PFB8, Polycarbonate membranes, 25x80mm, Neuro Probe) into the lower chamber.
186 A solution containing the chemokine (0, 10, 100, 1,000 ng/ml CXCL12) was placed below the
187 cell-permeable membrane. After a 3-h incubation in 5% CO₂ at 37 °C, the cells that had
188 migrated through the 8- μ m filter membrane were fixed, stained, and counted in three separate
189 fields ($\times 400$) by a microscope.

190

191 **Cell Invasion Assay**

192 Invasion assays were performed using a transwell chamber inserted with a polycarbonic
193 membrane (cat. 3422 Corning, USA). To reproduce appropriate in vivo environments for 2D and
194 3D cell movements, we added 80 μ l of extracellular matrix (Corning 356234) into the upper
195 compartment of the transwell cell culture inserts. CXCL12 (0, 10, 100, 1,000 ng/ml) was added
196 to the lower well of the plates as an attractant. 2×10^4 cells suspended in 100 μ l serum-free
197 medium were seeded into the upper chamber. The plates were incubated for 24 h at 37 °C. Then,
198 the cells on the lower side of the insert membrane were fixed. Finally, the cells on the lower side
199 of the filter were counted under a microscope.

200

201 **Adhesion Assay**

202 Briefly, a fibronectin (Sigma-Aldrich Corporation) solution was previously prepared and stored at
203 4 °C. Then, 96-well plates (Costar-3599, Corning, US) were coated with fibronectin (10 µg/ml in
204 PBS) at room temperature for 1 h. After coating, the fibronectin solution was removed. Thermally
205 denatured BSA was added to the plates, followed by an incubation of 1 h at 37 °C. Then, the plates
206 were washed twice with serum-free RPMI 1640 medium. CXCL12 (0, 10, 100, and 1,000 ng/ml)
207 was added to the wells of fibronectin-coated plates. After the addition of the prepared 100 µl cell
208 suspension (5×10^5 cells per ml), the plates were incubated at 37 °C for 30 min and then washed
209 thrice with PBS to remove non-adherent cells. Next, a 10 µl Cell Counting Kit-8 (CCK-8) solution
210 (Dojindo, Japan) was added to each well and incubated for 1.5 h. Finally, the adherent cells were
211 stained and quantified at OD450 using a Microplate Reader (Thermo) according to the
212 manufacturer's instructions. The cell adhesion ratio of the assay was calculated according to the
213 following formula: cell adhesion (%) = OD of the adhered cells /OD of the total cells \times 100%.

214

215 **F-actin Polymerization Assay**

216 Cellular F-actin measurement was done as described by Tsuboi (Tsuboi 2006). Pancreatic cancer
217 cells were stimulated with 100 ng/ml CXCL12 for the designated time points at 37 °C. Then, the
218 cells were fixed with 4% paraformaldehyde, permeabilized with 0.1% Triton X-100, and stained
219 with Alexa Fluor 568-phalloidin (Invitrogen) for 60 min at room temperature. The level of F-
220 actin was measured by a microplate fluorescence reader. The results were expressed as relative
221 F-actin values, as follows:

222
$$\text{F-actin } t/\text{F-actin } 0 = (\text{fluorescence } t/\text{mg ml}^{-1})/(\text{fluorescence } t_0/\text{mg ml}^{-1}).$$

223

224 **Statistical Analysis**

225 The statistical analyses were performed with GraphPad Prism 8 (La Jolla, CA, USA). The
226 experimental data are expressed as the mean \pm SD. We designed each experiment with 3
227 replicates, which were done all at the same time. And each experiment was performed three
228 times. One-way and two-way ANOVA were used to analyze the data. A p value below 0.05 was
229 considered statistically significant.

230

231 **Results**

232

233 **Role of ELMO2 in the Migration and Chemotaxis of Pancreatic Cancer Cells**

234 To explore the role played by ELMO2 in the process of cell migration, we initially investigated
235 its expression level in pancreatic cancer cell lines. The reasons why PANC-1 and AsPC-1 were
236 chosen in this study were as follows: Firstly, information concerning the clinical course of the
237 sites where cell lines were derived from was important in defining the biologic and pathologic
238 characteristics of the tumor cell lines. Both these two cell lines were derived from patients with
239 an adenocarcinoma in the head of the pancreas and they shared similar phenotypic
240 characteristics, such as adhesion, invasion and migration. Secondly, the cell population doubling

241 times for PANC-1 and AsPC-1 were very close which made it more convenient for our
242 experimental operation. Small interfering RNA (siRNA) was used to suppress ELMO2
243 expression (Figure 1A). Then, a wound-healing assay was utilized to evaluate cell migration. The
244 decreased expression of ELMO2 reduced the migration capacity of PANC-1 and AsPC-1 cells
245 (Figure 1C). Moreover, a chemotaxis assay indicated that CXCL12 could distinctly enhance the
246 chemotactic ability of PANC-1 and AsPC-1 cells, while ELMO2 silencing inhibited the
247 CXCL12-induced chemotaxis in these cell lines (Figure 1B).

248

249 **Knockdown of ELMO2 Inhibited Invasion, Adhesion, and F-actin Polymerization in** 250 **PANC-1 and AsPC-1 Cells**

251 Next, a cell invasion assay was performed to monitor the movement of pancreatic cancer cells
252 through an extracellular matrix. We found that ELMO2 knockdown suppressed CXCL12-
253 induced invasiveness in both PANC-1 and AsPC-1 cells (Figure 2A). Furthermore, cell adhesion
254 assay suggested that ELMO2 downregulation by siRNA weakened the adhesion ability of
255 PANC-1 and AsPC-1 cells (Figure 2B). When CXCL12 combines with its receptor CXCR4,
256 intracellular signaling events induce membrane protrusions because of actin polymerization.
257 These events enhance the motility of cancer cells and promote chemotaxis and invasion.
258 CXCL12 generated a transient F-actin accumulation in PANC-1 and AsPC-1 cells, in line with
259 previous findings (Yan et al. 2012). Notably, F-actin filaments were clearly reduced in siELMO2
260 cells within 30 s (Figure 2C). These results suggested that ELMO2 knockdown inhibited F-actin
261 polymerization in pancreatic cancer cells. Thus, ELMO2 might participate in CXCL12-mediated
262 invasion.

263

264 **ELMO2 Interacts with Gai2**

265 Previous reports have shown that the association between ELMO1 and Gai2 contributes to actin
266 polymerization in human breast cancer cells. Thus, it was reasonable to expect that Gai2
267 interacts with ELMO2 in pancreatic cancer cells. To verify this possibility, a Co-IP assay was
268 performed. First, exogenous overexpression of ELMO2 was successfully induced by transfecting
269 PANC-1 cells with the GV362-ELMO2-Flag plasmid. Then, ELMO2-Flag, along with its
270 endogenous interactors, was captured from PANC-1 cell lysates using specific anti-Flag
271 antibody. Interestingly, Gai2 was found among the ELMO2-interacting partners, as assessed by
272 immunoblotting with Gai2 antibody (Figure 3A). Moreover, when Gai2-Flag was overexpressed
273 following cell transfection with the GV141-GNAI2-Flag plasmid, endogenous ELMO2 was co-
274 precipitated by the anti-Flag antibody along with Gai2-Flag (Figure 3B). Taken together, our
275 results confirmed the physical association between ELMO2 and Gai2 in pancreatic cancer cells.

276

277 **Cell Stimulation with CXCL12 Results in ELMO2 Membrane Translocation**

278 To further investigate the interaction networks involving ELMO2 and Gai2,
279 immunofluorescence microscopy was used to examine the subcellular localization of the two
280 proteins. In unstimulated cells, clear Gai2-specific fluorescence, but not ELMO2 fluorescence,
281 was detected at the plasma membrane. Interestingly, after CXCL12 stimulation, ELMO2 was

282 also detected on the plasma membrane. According to the colocalization analysis performed on a
283 pixel by pixel basis, *Gai2* and ELMO2 were clearly found to co-localize on the plasma
284 membrane after CXCL12 stimulation of pancreatic cancer cells (Figure 4A). Next, the impact of
285 *Gai2* silencing on ELMO2 localization, and vice versa was explored in PANC-1 cells transfected
286 with the appropriate siRNAs (Figure 4B,C). Interestingly, the membrane translocation of
287 ELMO2 was reduced in *Gai2*-knockdown cells, even in the presence of CXCL12 stimulation,
288 while ELMO2 knockdown had no significant impact on the level of plasma membrane *Gai2*
289 (Figure 4C,D). Thus, *Gai2* might be a key factor for chemokine-induced ELMO2 recruitment to
290 the plasma membrane.

291

292 Discussion

293 Pancreatic cancer is one of the most malignant cancers, causing high morbidity and mortality.
294 This is due to the intrinsic characteristics of this malignancy, such as rapid tissue invasion and
295 metastasis. To acquire invasive and metastatic capabilities, cancer cells need to undergo multiple
296 cellular changes, including oncogene-triggered signaling cascades. Several proteins are involved
297 in these changes at the genetic and biochemical levels. ELMO family proteins are orthologs of *C.*
298 *elegans* CED-12. They possess no catalytic activity, but associate with other proteins, serving as
299 upstream activators and regulators of cytoskeletal rearrangements, thus favoring cell motility.
300 Several studies have suggested a role of ELMO proteins in cancer. For instance, ELMO1 was
301 clearly related to the invasive phenotype of glioma cells. In addition, the migratory and invasive
302 abilities of glioma cells increase with the level of ELMO1 expression. Other studies have
303 demonstrated that the overexpression of ELMO1 promotes cell motility and invasion in
304 hepatocellular carcinoma and serous ovarian cancer (Li et al. 2019; Wang et al. 2014). ELMO3
305 has also been reported to participate in events related to metastasis in several types of cancer,
306 including lung cancer, colorectal cancer, and squamous-cell carcinoma of the head and neck (Fan
307 et al. 2015; Kadletz et al. 2017; Peng et al. 2016). However, the function of ELMO2 in
308 pancreatic cancer progression and metastasis has been poorly investigated. During the
309 chemotaxis assay, a permeable filter separated the upper and lower wells of the Neuro Probe
310 AP48 chemotaxis chamber. Interestingly, cell migration through the permeable filter could be
311 inhibited when ELMO2 was reduced. Based on our data, the decrease in the number of migrated
312 cells under ELMO2 knockdown condition without CXCL12 stimulation was statistically
313 significant. The possible reason for this was that the decreased expression of ELMO2 reduced
314 the migration capacity of tumor cells. In this study, we showed that ELMO2 knockdown inhibits
315 CXCL12-mediated migration, chemotaxis, adhesion, and invasion of pancreatic cancer cells.
316 CXCL12 interaction with its receptor, CXCR4, causes intracellular actin polymerization, which
317 is necessary for pancreatic cancer cell migration and invasion. We found that stimulation with
318 CXCL12 induces a noticeable increase in F-actin in pancreatic cancer cells, which can be
319 prevented by ELMO2 knockdown. Therefore, ELMO2 is a boosting factor for the migration and
320 metastasis of pancreatic cancer cells. Further studies will be needed to exhaustively characterize
321 pathologically relevant ELMO2 interactions with other proteins.

322 During the past few years, extensive efforts have been made to identify potential interactors of
323 ELMO proteins. It has been reported that brain-specific angiogenesis inhibitor (BAI3), a G
324 protein-coupled receptor binding to ELMO1, regulated myoblast fusion (Hamoud et al. 2014).
325 Moreover, a member of the Nck protein family, Nck-1, interacts with ELMO1 and controls the
326 activity of the Rho family GTPase, Rac1, which is involved in the reorganization of the actin
327 cytoskeleton. Furthermore, the membrane-bound proteins Gai2 and Gβγ have been found to
328 associate with ELMO1. These proteins activate downstream signaling factors that have an
329 impact on the restructuring of the actin cytoskeleton and promote the migration of cancer cells.
330 However, the mechanism by which ELMO2 interaction with its putative partner, Gai2, affects
331 the process of metastasis has not been investigated in pancreatic cancer. In this study, co-
332 immunoprecipitation experiments demonstrated that exogenous ELMO2 directly interacted with
333 endogenous Gai2, and vice versa. Interestingly, we found that the expression of GNAI2 had
334 increased in the GV362-ELMO2 condition and when we overexpressed GNAI2 it seemed that
335 also the expression level of ELMO2 increased. Overexpression of ELMO2 or Gai2 might force
336 tumor cells to generate more endogenous Gai2 or ELMO2 to interact with in order to work
337 together for directing migration and invasion of cancer. Future studies are needed to understand
338 how these two proteins influence over the expression of one another. The interaction of ELMO2
339 with Gai2 was enhanced by CXCL12 stimulation. Moreover, CXCL12 stimulation promoted
340 Gai2-mediated membrane translocation of ELMO2. Interestingly, when the expression of Gai2
341 was suppressed in human pancreatic cancer cell line PANC-1, ELMO2 translocation was
342 substantially reduced, even in the presence of CXCL12 stimulation. It was suggested that Gai2
343 plays an indispensable role in ELMO2 translocation to the plasma membrane. Our results
344 confirmed this finding and demonstrated that a physiologically relevant interaction between
345 ELMO2 and Gai2 promoted actin polymerization in pancreatic cancer cells. We thus
346 hypothesize that CXCL12 binding to the G-protein-coupled receptor, CXCR4, triggered a signal
347 that was transmitted to the cell interior, causing ELMO2 recruitment to the plasma membrane.
348 The latter event was dependent on Gai2. Thus, intracellular signals generated by the newly
349 assembled CXCL12/ CXCR4 protein complex resulted in actin polymerization and invasive cell
350 migration.

351 In summary, we showed that ELMO2 plays an essential role in CXCL12-mediated chemotaxis,
352 migration, and invasion of human pancreatic cancer lines. Gai2 interacted directly with ELMO2
353 to promote metastatic changes. Considering these results, ELMO2 may be regarded as a
354 promising target for the treatment of pancreatic cancer metastasis. Further research is needed to
355 uncover the role of ELMO-related signaling in different types of cancer, identify valuable
356 prognostic biomarkers, and develop therapeutic strategies centered on ELMO signaling.
357

358 **Acknowledgments**

359 We are much obliged to Professor Rong Wang (Central Laboratory, Xuan Wu Hospital, Capital
360 Medical University), who kindly offered an experimental platform for our scientific research and
361 provided proofreading assistance for this article.

362

Funding

364 This work was supported by Beijing Hospitals Authority Youth Programme [grant number
365 QMS20180805]; Cultivate Foundation of Capital Medical University [grant number
366 PYZ2018154]; Top-notch Youth Project of the Supporting Plan for the Construction of High-
367 level Teachers in Beijing-affiliated Universities [grant number CIT&TCD201904093]; Beijing
368 Municipal Commission of Science and Technology [grant number Z171100001017077]; Beijing
369 Municipal Administration of Hospitals Clinical Medicine Development of Special Funding
370 Support [grant number XMLX201404].

371

Declaration of Interest: None

373

References

- 375 Archibald KM, Kulbe H, Kwong J, Chakravarty P, Temple J, Chaplin T, Flak MB, McNeish IA, Deen S, Brenton JD,
376 Young BD, and Balkwill F. 2012. Sequential genetic change at the TP53 and chemokine receptor CXCR4
377 locus during transformation of human ovarian surface epithelium. *Oncogene* 31:4987-4995.
378 10.1038/onc.2011.653
- 379 Balkwill F. 2004. Cancer and the chemokine network. *Nat Rev Cancer* 4:540-550. 10.1038/nrc1388
- 380 Condeelis J, and Segall JE. 2003. Intravital imaging of cell movement in tumours. *Nat Rev Cancer* 3:921-930.
381 10.1038/nrc1231
- 382 Condeelis J, Singer RH, and Segall JE. 2005. The great escape: when cancer cells hijack the genes for chemotaxis
383 and motility. *Annu Rev Cell Dev Biol* 21:695-718. 10.1146/annurev.cellbio.21.122303.120306
- 384 Conroy T, Bachet JB, Ayav A, Hugué F, Lambert A, Caramella C, Marechal R, Van Laethem JL, and Ducreux M. 2016.
385 Current standards and new innovative approaches for treatment of pancreatic cancer. *Eur J Cancer* 57:10-
386 22. 10.1016/j.ejca.2015.12.026
- 387 Fan W, Yang H, Xue H, Sun Y, and Zhang J. 2015. ELMO3 is a novel biomarker for diagnosis and prognosis of non-
388 small cell lung cancer. *Int J Clin Exp Pathol* 8:5503-5508.
- 389 Fraser CC. 2008. G protein-coupled receptor connectivity to NF-kappaB in inflammation and cancer. *Int Rev*
390 *Immunol* 27:320-350. 10.1080/08830180802262765
- 391 Fritsch R, de Krijger I, Fritsch K, George R, Reason B, Kumar MS, Diefenbacher M, Stamp G, and Downward J. 2013.
392 RAS and RHO families of GTPases directly regulate distinct phosphoinositide 3-kinase isoforms. *Cell*
393 153:1050-1063. 10.1016/j.cell.2013.04.031
- 394 Garrido-Laguna I, and Hidalgo M. 2015. Pancreatic cancer: from state-of-the-art treatments to promising novel
395 therapies. *Nat Rev Clin Oncol* 12:319-334. 10.1038/nrclinonc.2015.53
- 396 Gumienny TL, Brugnera E, Tosello-Tramont AC, Kinchen JM, Haney LB, Nishiwaki K, Walk SF, Nemergut ME,
397 Macara IG, Francis R, Schedl T, Qin Y, Van Aelst L, Hengartner MO, and Ravichandran KS. 2001. CED-
398 12/ELMO, a novel member of the CrkII/Dock180/Rac pathway, is required for phagocytosis and cell
399 migration. *Cell* 107:27-41. 10.1016/s0092-8674(01)00520-7
- 400 Guyon A. 2014. CXCL12 chemokine and its receptors as major players in the interactions between immune and
401 nervous systems. *Front Cell Neurosci* 8:65. 10.3389/fncel.2014.00065
- 402 Hamoud N, Tran V, Croteau LP, Kania A, and Cote JF. 2014. G-protein coupled receptor BAI3 promotes myoblast

- 403 fusion in vertebrates. *Proc Natl Acad Sci U S A* 111:3745-3750. 10.1073/pnas.1313886111
- 404 Hu TH, Yao Y, Yu S, Han LL, Wang WJ, Guo H, Tian T, Ruan ZP, Kang XM, Wang J, Wang SH, and Nan KJ. 2014. SDF-
405 1/CXCR4 promotes epithelial-mesenchymal transition and progression of colorectal cancer by activation
406 of the Wnt/beta-catenin signaling pathway. *Cancer Lett* 354:417-426. 10.1016/j.canlet.2014.08.012
- 407 Hurst JH, and Hooks SB. 2009. Regulator of G-protein signaling (RGS) proteins in cancer biology. *Biochem*
408 *Pharmacol* 78:1289-1297. 10.1016/j.bcp.2009.06.028
- 409 Iglesias PA, and Devreotes PN. 2008. Navigating through models of chemotaxis. *Curr Opin Cell Biol* 20:35-40.
410 10.1016/j.ceb.2007.11.011
- 411 Jarzynka MJ, Hu B, Hui KM, Bar-Joseph I, Gu W, Hirose T, Haney LB, Ravichandran KS, Nishikawa R, and Cheng SY.
412 2007. ELMO1 and Dock180, a bipartite Rac1 guanine nucleotide exchange factor, promote human glioma
413 cell invasion. *Cancer Res* 67:7203-7211. 10.1158/0008-5472.CAN-07-0473
- 414 Jiang J, Liu G, Miao X, Hua S, and Zhong D. 2011. Overexpression of engulfment and cell motility 1 promotes cell
415 invasion and migration of hepatocellular carcinoma. *Exp Ther Med* 2:505-511. 10.3892/etm.2011.229
- 416 Jin T, Xu X, Fang J, Isik N, Yan J, Brzostowski JA, and Hereld D. 2009. How human leukocytes track down and destroy
417 pathogens: lessons learned from the model organism Dictyostelium discoideum. *Immunol Res* 43:118-127.
418 10.1007/s12026-008-8056-7
- 419 Kadletz L, Heiduschka G, Wiebringhaus R, Gurnhofer E, Kotowski U, Haymerle G, Brunner M, Barry C, and Kenner L.
420 2017. ELMO3 expression indicates a poor prognosis in head and neck squamous cell carcinoma - a short
421 report. *Cell Oncol (Dordr)* 40:193-198. 10.1007/s13402-016-0310-8
- 422 Kim M, Kim M, Lee S, Kuninaka S, Saya H, Lee H, Lee S, and Lim DS. 2013. cAMP/PKA signalling reinforces the LATS-
423 YAP pathway to fully suppress YAP in response to actin cytoskeletal changes. *EMBO J* 32:1543-1555.
424 10.1038/emboj.2013.102
- 425 Kleeff J, Korc M, Apte M, La Vecchia C, Johnson CD, Biankin AV, Neale RE, Tempero M, Tuveson DA, Hruban RH,
426 and Neoptolemos JP. 2016. Pancreatic cancer. *Nat Rev Dis Primers* 2:16022. 10.1038/nrdp.2016.22
- 427 Li H, Wang Y, Lu Y, and Li F. 2019. Annexin A2 interacting with ELMO1 regulates HCC chemotaxis and metastasis.
428 *Life Sci* 222:168-174. 10.1016/j.lfs.2019.03.003
- 429 Li H, Yang L, Fu H, Yan J, Wang Y, Guo H, Hao X, Xu X, Jin T, and Zhang N. 2013. Association between Galphai2 and
430 ELMO1/Dock180 connects chemokine signalling with Rac activation and metastasis. *Nat Commun* 4:1706.
431 10.1038/ncomms2680
- 432 Li X, Li P, Chang Y, Xu Q, Wu Z, Ma Q, and Wang Z. 2014. The SDF-1/CXCR4 axis induces epithelial-mesenchymal
433 transition in hepatocellular carcinoma. *Mol Cell Biochem* 392:77-84. 10.1007/s11010-014-2020-8
- 434 Muller A, Homey B, Soto H, Ge N, Catron D, Buchanan ME, McClanahan T, Murphy E, Yuan W, Wagner SN, Barrera
435 JL, Mohar A, Verastegui E, and Zlotnik A. 2001. Involvement of chemokine receptors in breast cancer
436 metastasis. *Nature* 410:50-56. 10.1038/35065016
- 437 Murphy PM. 2001. Chemokines and the molecular basis of cancer metastasis. *N Engl J Med* 345:833-835.
438 10.1056/NEJM200109133451113
- 439 Patel M, Pelletier A, and Cote JF. 2011. Opening up on ELMO regulation: New insights into the control of Rac
440 signaling by the DOCK180/ELMO complex. *Small GTPases* 2:268-275. 10.4161/sgtp.2.5.17716
- 441 Peng HY, Yu QF, Shen W, Guo CM, Li Z, Zhou XY, Zhou NJ, Min WP, and Gao D. 2016. Knockdown of ELMO3
442 Suppresses Growth, Invasion and Metastasis of Colorectal Cancer. *Int J Mol Sci* 17. 10.3390/ijms17122119
- 443 Siegel RL, Miller KD, and Jemal A. 2018. Cancer statistics, 2018. *CA Cancer J Clin* 68:7-30. 10.3322/caac.21442

- 444 Sun R, Gao P, Chen L, Ma D, Wang J, Oppenheim JJ, and Zhang N. 2005. Protein kinase C zeta is required for
445 epidermal growth factor-induced chemotaxis of human breast cancer cells. *Cancer Res* 65:1433-1441.
446 10.1158/0008-5472.CAN-04-1163
- 447 Swaney KF, Huang CH, and Devreotes PN. 2010. Eukaryotic chemotaxis: a network of signaling pathways controls
448 motility, directional sensing, and polarity. *Annu Rev Biophys* 39:265-289.
449 10.1146/annurev.biophys.093008.131228
- 450 Toret CP, Collins C, and Nelson WJ. 2014. An Elmo-Dock complex locally controls Rho GTPases and actin
451 remodeling during cadherin-mediated adhesion. *J Cell Biol* 207:577-587. 10.1083/jcb.201406135
- 452 Tsuboi S. 2006. A complex of Wiskott-Aldrich syndrome protein with mammalian verprolins plays an important role
453 in monocyte chemotaxis. *J Immunol* 176:6576-6585. 10.4049/jimmunol.176.11.6576
- 454 Wang J, Dai JM, Che YL, Gao YM, Peng HJ, Liu B, Wang H, and Linghu H. 2014. Elmo1 helps dock180 to regulate
455 Rac1 activity and cell migration of ovarian cancer. *Int J Gynecol Cancer* 24:844-850.
456 10.1097/IGC.000000000000137
- 457 Xu X, Meckel T, Brzostowski JA, Yan J, Meier-Schellersheim M, and Jin T. 2010. Coupling mechanism of a GPCR and
458 a heterotrimeric G protein during chemoattractant gradient sensing in Dictyostelium. *Sci Signal* 3:ra71.
459 10.1126/scisignal.2000980
- 460 Yan J, Mihaylov V, Xu X, Brzostowski JA, Li H, Liu L, Veenstra TD, Parent CA, and Jin T. 2012. A Gbetagamma
461 effector, ElmoE, transduces GPCR signaling to the actin network during chemotaxis. *Dev Cell* 22:92-103.
462 10.1016/j.devcel.2011.11.007
- 463 Yang P, Wang G, Huo H, Li Q, Zhao Y, and Liu Y. 2015. SDF-1/CXCR4 signaling up-regulates survivin to regulate
464 human sacral chondrosarcoma cell cycle and epithelial-mesenchymal transition via ERK and PI3K/AKT
465 pathway. *Med Oncol* 32:377. 10.1007/s12032-014-0377-x
- 466 Zhang B, Shi L, Lu S, Sun X, Liu Y, Li H, Wang X, Zhao C, Zhang H, and Wang Y. 2015. Autocrine IL-8 promotes F-actin
467 polymerization and mediate mesenchymal transition via ELMO1-NF-kappaB-Snail signaling in glioma.
468 *Cancer Biol Ther* 16:898-911. 10.1080/15384047.2015.1028702
- 469 Zhang G, Chen X, Qiu F, Zhu F, Lei W, and Nie J. 2014. A novel interaction between the SH2 domain of signaling
470 adaptor protein Nck-1 and the upstream regulator of the Rho family GTPase Rac1 engulfment and cell
471 motility 1 (ELMO1) promotes Rac1 activation and cell motility. *J Biol Chem* 289:23112-23122.
472 10.1074/jbc.M114.549550

473

474 Figure Legends

475

476 Fig. 1. Function of ELMO2 in pancreatic cancer cell migration and chemotaxis. (A)

477 Western blot shows an evident knockdown of ELMO2 in human pancreatic cell lines. GAPDH

478 was used as a loading control for western blot. (B) Chemotaxis in ELMO2 knockdown cells

479 (data are the mean of three independent experiments; two-way ANOVA, $**p < 0.001$). (C)

480 Wound healing assay in siELMO2 cells. Pancreatic cancer cells were seeded in 6-well plates and
481 incubated until the monolayer reached 80-90% confluence (ca. 24 h of growth). The medium was

482 replaced by an RPMI 1640 medium containing 1% fetal bovine serum. The gap distance was

483 measured at 0, 3, 6, 9, 12, and 24 h (data are the mean of three independent experiments; two-

484 way ANOVA, $**p < 0.001$).

485

486 **Fig. 2. Knockdown of ELMO2 inhibited F-actin polymerization and invasion in pancreatic**
487 **cancer cells.** (A) The invasion assay showed that ELMO2 knockdown decreased the CXCL12-
488 mediated invasive abilities of PANC-1 and AsPC-1 cells (data are the mean of three independent
489 experiments; two-way ANOVA, $**p < 0.001$). (B) Adhesion assay in PANC-1 and AsPC-1 cells.
490 The cell adhesion rate was much higher in normal cells than in siELMO2 cells (data are the
491 mean of three independent experiments; two-way ANOVA, $**p < 0.001$). (C) ELMO2
492 knockdown reduced actin polymerization in pancreatic cancer cells. F-actin value was measured
493 at different time points (0, 4, 8, 15, 30, 60, 120, and 300 s). Time course of relative F-actin
494 content in normal, control, and siELMO2 cells upon CXCL12 stimulation (data are the mean of
495 three independent experiments; two-way ANOVA, $**p < 0.001$).

496

497 **Fig. 3. ELMO2 interacts with Gai2.** (A) PANC-1 cells were transfected with GV362 Flag-
498 ELMO2 to increase ELMO2 expression. Cell lysates were immunoprecipitated with anti-Flag
499 antibody, and magnetic beads were used to capture the immune complexes. The eluted proteins
500 were separated by SDS-PAGE and detected with specific antibodies. (B) Exogenous Gai2 was
501 overexpressed by transfection with the GV141-GNAI2-Flag plasmid. Proteins of the immune
502 complex were pulled down by anti-Flag antibody and detected by anti-ELMO2 or anti-Gai2
503 antibodies. Input was the total protein lysates which were prepared from cells with RIPA lysis
504 buffer. IP referred to the immunoprecipitate that was eluted from the beads after the
505 immunoprecipitation.

506

507 **Fig. 4. CXCL12 stimulation results in ELMO2 membrane translocation.** (A) Plasma
508 membrane colocalizations of Gai2 and ELMO2 were evident upon pancreatic cancer cell
509 stimulation with CXCL12. The extent of colocalization was calculated through ImageJ software.
510 (B) No significant changes in plasma membrane-associated Gai2 fluorescence were detected in
511 ELMO2 knockdown cells, even with CXCL12 stimulation. One-way ANOVA, $p > 0.05$. (C)
512 Western blot clearly shows the Gai2 knockdown in siRNA-transfected PANC-1 cells. GAPDH
513 was used as a loading control. (D) ELMO2 membrane translocation was reduced in Gai2
514 knockdown cells, even in the presence of CXCL12 stimulation. Twenty-five images were
515 analyzed by ImageJ software. One-way ANOVA, $**p < 0.001$. The arrows indicated the plasma
516 membrane colocalization of Gai2 or ELMO2.

Figure 1

Function of ELMO2 in pancreatic cancer cell migration and chemotaxis.

(A) Western blot shows an evident knockdown of ELMO2 in human pancreatic cell lines. GAPDH was used as a loading control for western blot. (B) Chemotaxis in ELMO2 knockdown cells (data are the mean of three independent experiments; two-way ANOVA, $**p < 0.001$). (C) Wound healing assay in siELMO2 cells. Pancreatic cancer cells were seeded in 6-well plates and incubated until the monolayer reached 80-90% confluence (ca. 24 h of growth). The medium was replaced by an RPMI 1640 medium containing 1% fetal bovine serum. The gap distance was measured at 0, 3, 6, 9, 12, and 24 h (data are the mean of three independent experiments; two-way ANOVA, $**p < 0.001$).

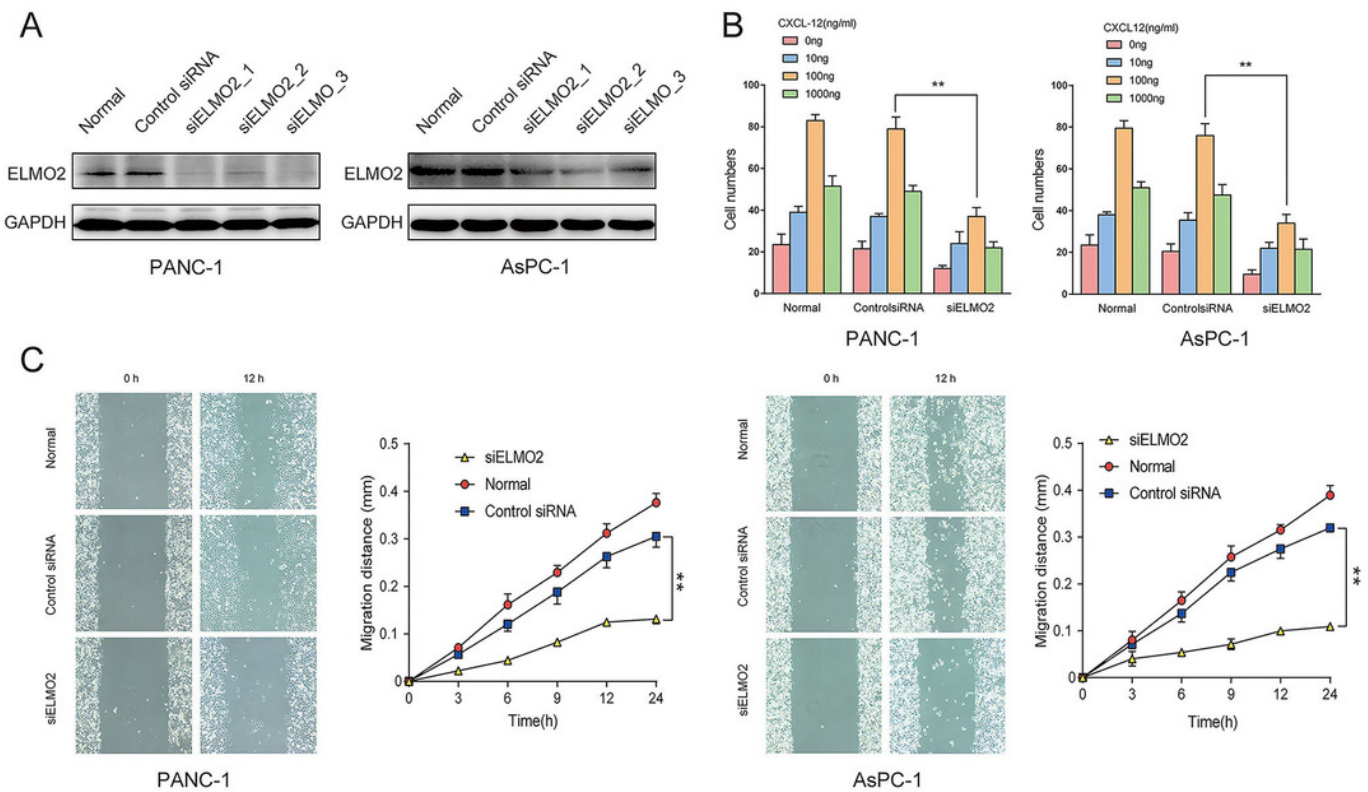
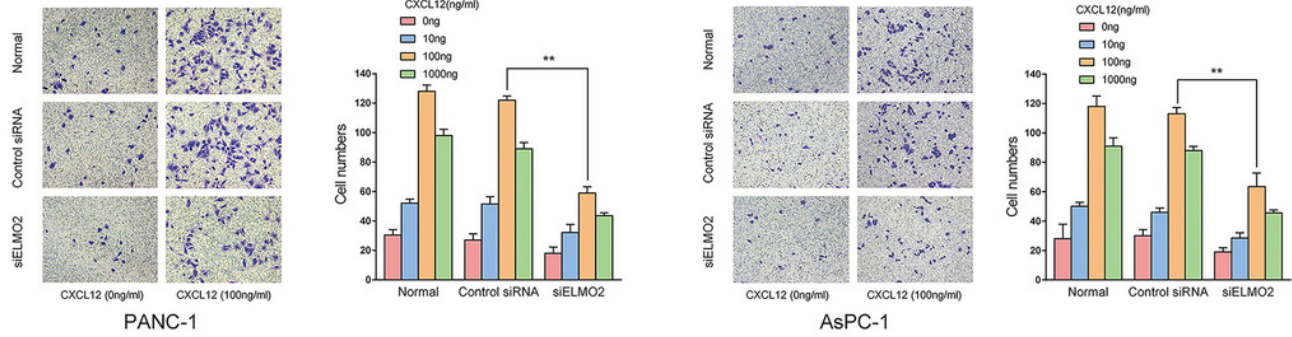


Figure 2

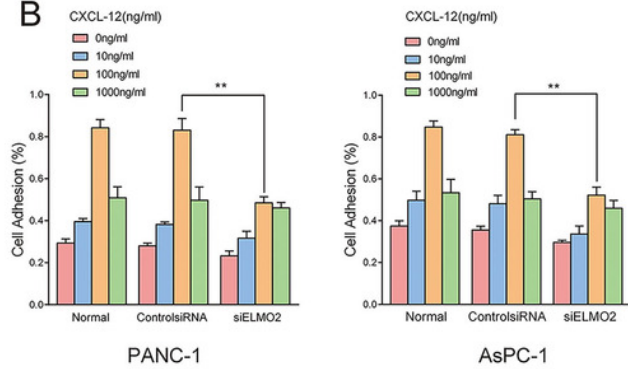
Knockdown of ELMO2 inhibited F-actin polymerization and invasion in pancreatic cancer cells.

(A) The invasion assay showed that ELMO2 knockdown decreased the CXCL12-mediated invasive abilities of PANC-1 and AsPC-1 cells (data are the mean of three independent experiments; two-way ANOVA, $**p < 0.001$). (B) Adhesion assay in PANC-1 and AsPC-1 cells. The cell adhesion rate was much higher in normal cells than in siELMO2 cells (data are the mean of three independent experiments; two-way ANOVA, $**p < 0.001$). (C) ELMO2 knockdown reduced actin polymerization in pancreatic cancer cells. F-actin value was measured at different time points (0, 4, 8, 15, 30, 60, 120, and 300 s). Time course of relative F-actin content in normal, control, and siELMO2 cells upon CXCL12 stimulation (data are the mean of three independent experiments; two-way ANOVA, $**p < 0.001$).

A



B



C

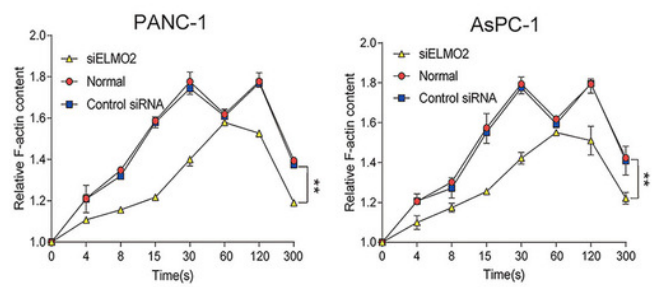


Figure 3

ELMO2 interacts with G α i2.

(A) PANC-1 cells were transfected with GV362 Flag-ELMO2 to increase ELMO2 expression. Cell lysates were immunoprecipitated with anti-Flag antibody, and magnetic beads were used to capture the immune complexes. The eluted proteins were separated by SDS-PAGE and detected with specific antibodies. (B) Exogenous G α i2 was overexpressed by transfection with the GV141-GNAI2-Flag plasmid. Proteins of the immune complex were pulled down by anti-Flag antibody and detected by anti-ELMO2 or anti-G α i2 antibodies. Input was the total protein lysates which were prepared from cells with RIPA lysis buffer. IP referred to the immunoprecipitate that was eluted from the beads after the immunoprecipitation.

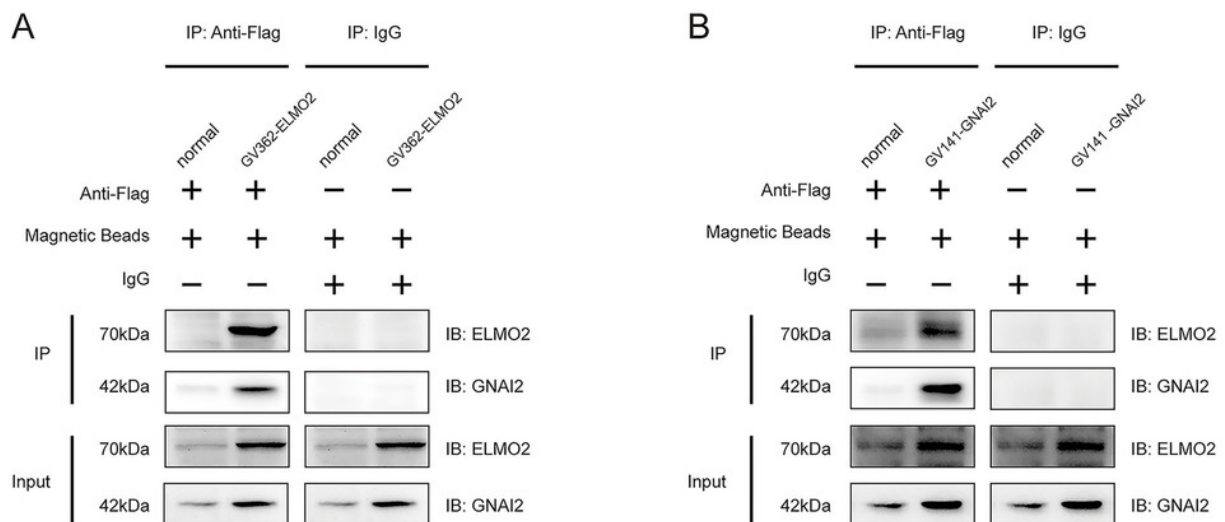


Figure 4

CXCL12 stimulation results in ELMO2 membrane translocation.

(A) Plasma membrane colocalizations of Gαi2 and ELMO2 were evident upon pancreatic cancer cell stimulation with CXCL12. The extent of colocalization was calculated through ImageJ software. (B) No significant changes in plasma membrane-associated Gαi2 fluorescence were detected in ELMO2 knockdown cells, even with CXCL12 stimulation. One-way ANOVA, $p > 0.05$. (C) Western blot clearly shows the Gαi2 knockdown in siRNA-transfected PANC-1 cells. GAPDH was used as a loading control. (D) ELMO2 membrane translocation was reduced in Gαi2 knockdown cells, even in the presence of CXCL12 stimulation. Twenty-five images were analyzed by ImageJ software. One-way ANOVA, $**p < 0.001$. The arrows indicated the plasma membrane colocalization of Gαi2 or ELMO2.

